Physica Scripta

PAPER

Mechanism of ion track formation in silicon by much lower energy deposition than the formation threshold

H Amekura[1,*], K Narumi[2], A Chiba[2], Y Hirano[2], K Yamada[2], S Yamamoto[2], N Ishikawa[3], N Okubo[3], M Toulemonde[4] and Y Saitoh[2]

[1] National Institute for Materials Science (NIMS), Tsukuba, Ibaraki 305-0003, Japan
[2] National Institutes for Quantum Science and Technology (QST), Takasaki, Gunma 370-1292, Japan
[3] Japan Atomic Energy Agency (JAEA), Tokai, Ibaraki 319-1195, Japan
[4] Centre de Recherche sur les Ions, les Matériaux et la Photonique, CIMAP-GANIL, Normandie University CEA, CNRS, Caen, 14000, France
[*] Author to whom any correspondence should be addressed.

E-mail: amekura.hiroshi@nims.go.jp

OPEN ACCESS

RECEIVED
13 October 2022

REVISED
27 January 2023

ACCEPTED FOR PUBLICATION
14 February 2023

PUBLISHED
6 March 2023

Keywords: C_{60} ion, ion track, swift heavy ion, silicon, synergy effect, track recrystallization

Abstract

Mechanism of the ion track formation in crystalline silicon (c-Si) is discussed, particularly under 1–9 MeV C_{60} ion irradiation. In this energy region, the track formation was not expected because the energy E was much lower than the threshold of $E_{th} = 17$ MeV determined by extrapolation from higher energy data in the past literature. The track formation is different between irradiations of C_{60} ions and of monoatomic ions: The tracks were observed under 3 MeV C_{60} ion irradiation but not under 200 MeV Xe ions, while both the irradiations have the same electronic stopping (S_e) of 14 keV nm^{-1} but much higher nuclear stopping (S_n) for the former ions. The involvement of S_n is suggested for the C_{60} ions. While the inelastic thermal spike (i-TS) calculations predict that the high energy monoatomic ion irradiation forms the tracks, the tracks have never been experimentally detected, suggesting quick annihilation of the tracks by highly enhanced recrystallization in c-Si. Exceptions are C_{60} ions of 1–9 MeV, where the track radii are well reproduced by the i-TS theory with assuming the melting transition. Collisional damage induced by the high S_n from C_{60} ions obstructs the recrystallization in c-Si. Then the tracks formed by the melting transition survive against the recrystallization. This is a new type of the synergy effect between S_e and S_n, different from the already-known mechanisms, i.e., the pre-damage effect and the unified thermal spike. While c-Si was believed as a radiation-hard material in the S_e regime with high S_e threshold, this study suggests that c-Si has a low S_e threshold but with efficient recrystallization.

1. Introduction

When a high energy heavy ion in the electronic stopping regime, i.e., swift heavy ion (SHI) [1–3], is injected into some solids, a damaged region of cylindrical shape with high aspect ratio is formed along the nearly straight trajectory of the ion, which is called a latent ion track [4, 5]. The track formation is governed by the electronic energy deposition processes. In fact, the diameters of the tracks increase with increasing the electronic energy deposition (S_e). However, the diameters exhibit threshold behaviors at low S_e, below which the tracks are no longer formed. The threshold value $S_{e,th}$ strongly depends on material species [6]. Limited but relatively many materials show the ion tracks [7].

According to the inelastic thermal spike (i-TS) model [8], the tracks are considered as regions transiently molten or vaporized by energy deposited from SHIs. The threshold is ascribed to the energy required for the melting or vaporization transition, i.e., the sum of latent heats and integrated heat capacities. However, it is recently pointed out that the track diameters are determined from not only the diameters of the molten/vaporized regions but also the recrystallization processes [9]. Furthermore, it is also pointed out that the track

formations by the synergy effects between S_e and the nuclear energy deposition (S_n) are observed in some materials [3, 10–12], while the track formation is mostly governed by S_e,

Crystalline silicon (c-Si) is one of the most important materials in today's technology. This material is known as a radiation-hard material in the electronic stopping regime: Any swift heavy *monoatomic* ions do not form ion tracks in c-Si, whatever high energy the ions have [13–15]. Toulemonde *et al* [13] studied the ion fluence dependence of the electric resistivity of c-Si under irradiations with various S_e between 3.7 keV nm^{-1} and 14 keV nm^{-1} and concluded that defect formation by electronic excitation is inefficient in c-Si. Mary *et al* evaluated c-Si irradiated with 3.5 GeV Xe ($S_e = 8.8$ keV nm^{-1}) [14] and 3.6 GeV U ions (23.7 keV nm^{-1}) [15] by the deep-level transient spectroscopy (DLTS), and concluded that the irradiations introduced point defects only, whose concentration was explained by the nuclear collisions only. Neither the track formation nor the point defect formation via the S_e process was observed. It should be noted that the 3.6 GeV U ions [15], which Mary *et al* utilized, was close to the Bragg peak, i.e., the highest S_e value in c-Si attainable by SHIs. However, it was still lower than the S_e threshold of the track formation in c-Si of ∼30 keV nm^{-1} [16].

Despite these observations, some scientists reported the track formations in c-Si with monoatomic SHIs, which were later regarded as uncertain. Furuno *et al* [17] formed Si films of 5 nm thick with the very small grain sizes of typically 1 nm by evaporation, irradiated them with 207 MeV Au ions ($S_e = 17$ keV nm^{-1}), and observed discontinuous tracks by TEM. Dunlop *et al* [18] criticized the observations since the Si films with the grain sizes of 1 nm show much different material properties from the bulk crystalline Si. Therefore, the work by Furuno *et al* evidences the track formation in Si nano-aggregates, but not in bulk crystalline Si. Furthermore, Itoh *et al* regarded in their paper that Furuno *et al* observed the track formation in amorphous Si, which was induced with lower S_e threshold than crystalline Si [6].

Srivastava *et al* irradiated c-Si wafers with 100 MeV Au ions ($S_e = 12$ keV nm^{-1}). They observed the surface craters by AFM [19] but not ion tracks directly, while the craters can be formed by the tracks. Because of the limited spatial resolution of AFM, the observed surface structures were typically ∼150 nm wide, while the track diameter of c-Si should be 10 nm wide or less. Since the evidence by Srivastava *et al* is indirect and ambiguous, it is not possible to conclude the track formation in c-Si.

The track formation in c-Si was succeeded in utilizing fullerene (C_{60}) ions, since a C_{60} ion provides much higher energy deposition than the heaviest monoatomic ions of U. Since all the sixty C atoms are injected into c-Si at the same time at almost the same position, i.e., within the diameter of C_{60} molecule of 0.7 nm, roughly sixty times greater energy is deposited than the carbon monoatomic ion does. To calculate the electronic and nuclear stopping power S_i ($i = e$ or n) of C_{60} ions at the energy E, i.e., $S_i(E, C_{60})$, a following relationship was assumed [20],

$$S_i(E,\ C_{60}) = 60\ S_i(E/60,\ C_1)\ (i = e\ or\ n) \tag{1}$$

where $S_i(E, C_1)$ denotes the S_i value of C monoatomic ions at the energy E, which is calculated from SRIM 2013 code [21].

In the late 1990s, Canut *et al* [22] and Dunlop *et al* [18] simultaneously succeeded in producing ion tracks in c-Si using 30 and 40 MeV C_{60} ions from the Orsay facility in France. With decreasing the energy from 40 MeV, 30 MeV, and to 20 MeV [16], the track mean diameter decreased from 10.5 nm, 8.4 nm, and to 6.0 nm. (For fair comparison, the S_e and S_n values of the Orsay irradiations were recalculated by SRIM 2013 [21] from the ion energy and equation (1), since the stopping powers depend on the version of SRIM code). The relationship between the squared track radii and the electronic stopping power S_e of C_{60} ions is plotted in figure 1. Straight lines in figure 1 indicate following relation:

$$R^2 = C(S_e - S_{e,th}) \tag{2}$$

where R, C, and $S_{e,th}$ denote the track radius, a proportional coefficient, and the S_e threshold, respectively. The relation (2) has been justified in other semiconductors of Ge, GaAs, and InP irradiated with C_{60} cluster ions [23].

From the Orsay data (open circles), the S_e threshold of ∼30 keV nm^{-1}, i.e., the C_{60} energy of 17 MeV, is extrapolated as shown in figure 1. Consequently, no track formation could be expected with C_{60} irradiations at 17 MeV and lower. However, as shown by closed symbols in figure 1, we have observed track formation under C_{60} irradiation at 1–6 MeV [24], which is much lower energy than the threshold of 17 MeV extrapolated from the Orsay data [16, 18, 22] . It should be noted again that the tracks were observed in c-Si even under 1 MeV C_{60} irradiation, while the track sizes decrease with the energy [24]. Following three observations also should be noted: (i) the mean track radius at 6 MeV (∼5 nm) is larger than that at 20 MeV (∼3 nm), while the latter has higher energy than the former. (ii) The tracks formed by the irradiations at $E \leqslant 6$ MeV also follow the relation (2), while the threshold $S_{e,th}$ is much lower as 4.2 keV nm^{-1} [24]. (iii) As clearly shown in figure 1, the S_e dependence of the track radii formed in Orsay and that in Takasaki do not overlap with each other. If both the data from Takasaki and from Orsay fall on the same curve, the track mean radii should decrease between 6 MeV and 20 MeV. It was one of the motivations for the additional irradiation at 9 MeV.

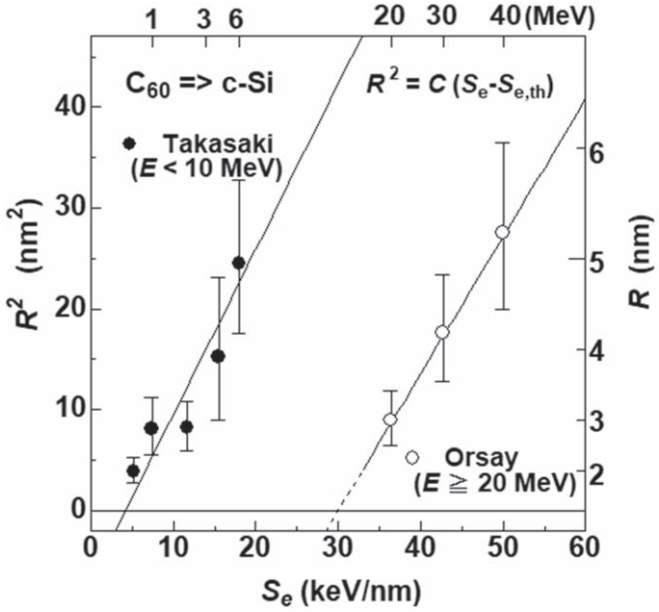

Figure 1. The electronic stopping power S_e dependence of squared track radii R^2 formed by C_{60} ion irradiations. Open and closed circles indicate the data observed in Orsay ($E = 20$–40 MeV) [16, 22] and Takasaki ($E \leqslant 6$ MeV) [24], respectively. For reference, the C_{60} ion energy and the track radius R are indicated in the top and right axes, respectively. Solid lines indicate relations fitted by the equation (2). Reproduced from [24] CC BY 4.0.

In this paper, the mechanism of this phenomenon, i.e., the track formation in c-Si with C_{60} ion irradiation of much lower energies of 1–9 MeV than the previously extrapolated threshold of 17 MeV, is discussed based on the data shown in the previous paper [24] and new data shown in this paper.

2. Experimental

Samples of single crystalline silicon were cut from commercially available Si wafers of p-type conduction (boron-doped) grown by the Czochralski method, with resistivity of ~1 Ω cm, surface orientation of <1 1 1>, and thickness of ~0.38 mm. The samples were mechanically cut into 3 mm × 4 mm rectangles, which are hereafter called bulk samples. The bulk samples were immersed in hydrofluoric acid to remove surface oxides. The tracks were observed by transmission electron microscopy (TEM). Two different configurations of TEM samples (pre-thinned and post-thinned) were prepared from the bulk samples. The pre-thinned samples were thinned down from a bulk sample with 30 keV Ga focused ion beam (FIB) milling to a thickness of ~100 nm, which were held on TEM grids. Then the pre-thinned samples on the TEM grids were irradiated by C_{60} ions with an incident angle of 7° from the surface normal, to evaluate the diameters of the tracks. In the case of the post-thinned samples, bulk samples were irradiated by C_{60} ions with the incident angle of 7° from the surface normal of the 3 mm × 4 mm face, and the cross-sectional samples were thinned down to a thickness of ~100 nm by FIB to observe the depth profiles of the ion tracks. See [24] for details. To identify the surface position of the post-thinned samples, a thin layer of Pt was deposited on the sample surface before the FIB milling.

Irradiation of C_{60} ions was conducted at the Takasaki Advanced Radiation Research Institute (TARRI), of the National Institutes for Quantum Science and Technology (QST), using a 3 MV tandem accelerator and a newly developed high-flux C_{60} negative ion source [25]. C_{60} ions with charge state of +1 (C_{60}^{+}) were utilized for 1–6 MeV irradiations, while those with +2 (C_{60}^{2+}) were utilized for 9 MeV irradiation. While the magnetic mass separation of ions was applied, it does not matter for singly charged ions. However, it is difficult for the doubly charged C_{60} ions to exclude the mixture of fragmented ions with the same m/q, i.e., 4.5 MeV C_{30}^{+} ions and 9 MeV C C_{60}^{2+} ions. However, evaluation of the beam with a semiconductor detector confirmed that the signal from 4.5 MeV C_{30}^{+} ions was almost negligible compared to 9 MeV C_{60}^{2+} ions.

The samples were mostly irradiated to low fluences of 5×10^{10}–1×10^{11} C_{60} cm^{-2} to avoid overlaps between the tracks. For precise control of the low fluence, the ion flux was reduced to below 50 pA through mesh-type attenuators and an aperture of 3 mm in diameter, while using the high-flux ion source [25]. The incident angle was set to 7° from the surface normal to avoid channeling effects. In fact, the channeling of C_{60} ions were observed in quartz (SiO_2) crystal, while the sizes of the crystal channels were smaller than those of C_{60} ions [26]. For comparison, some samples were irradiated with 200 MeV Xe^{14+} ions from the tandem accelerator in the Japan Atomic energy Agency (JAEA), Tokai Research and Development Center.

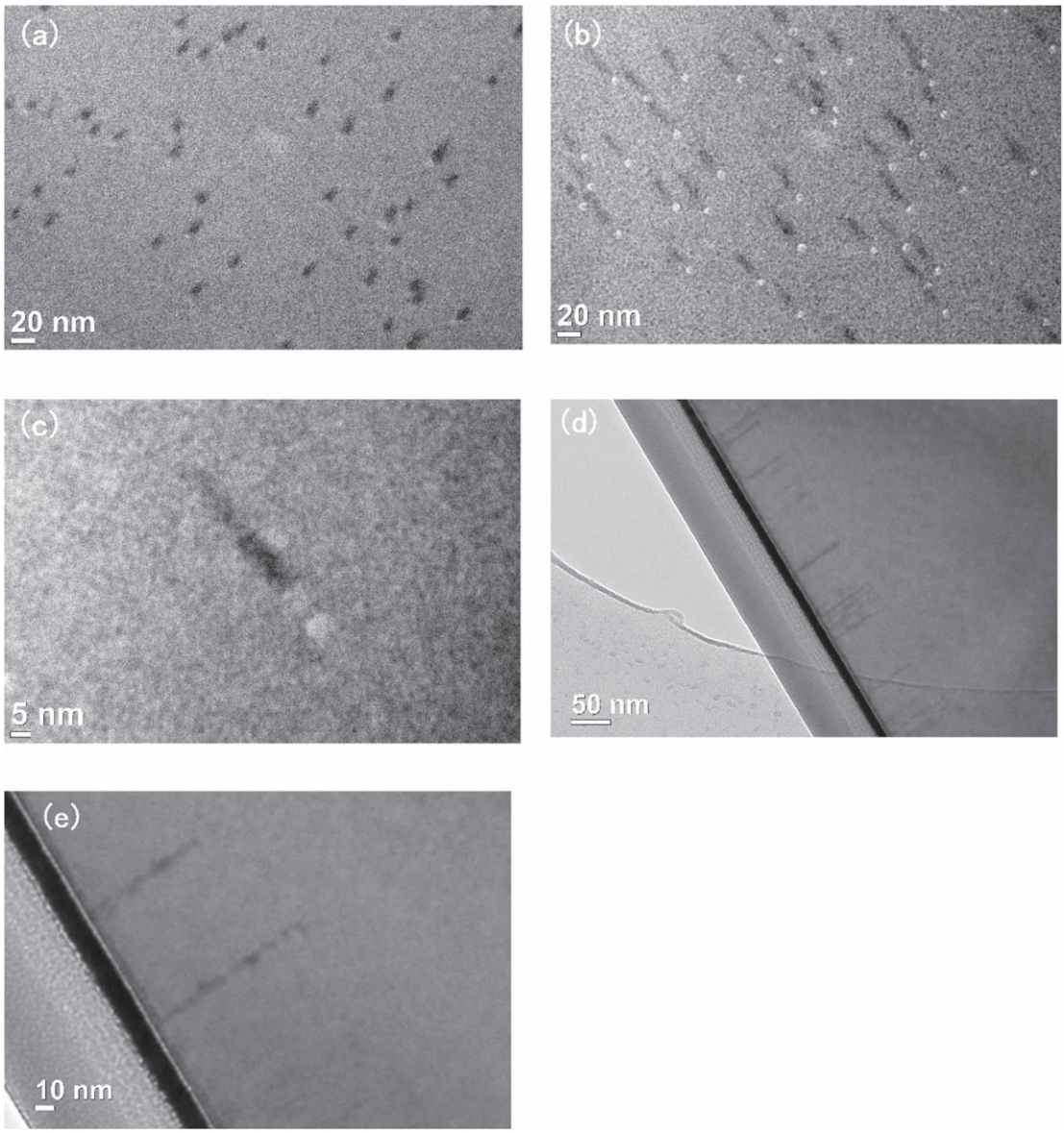

Figure 2. Bright field TEM images of ion tracks in c-Si formed by 9 MeV C_{60}^{2+} ion irradiations to the pre-thinned samples (a)-(c) and the post-thinned samples (d)(e). The observation angle was 0° for (a)(d)(e) and 30° for (b)(c) from the surface normal. Black thick layers in (d)(e) are deposited Pt layers for surface marker. In (b) and (c), the entrances and the main bodies of the tracks are visible as white circles and black rods, respectively. Less modified regions, i.e., gaps, are observed between the entrances and the main bodies as shown in (b)(c) but not in (d)(e).

TEM observation of the two different configurations (the pre- and the post-thinned) was conducted using a JEM-2100 microscope (JEOL) with an operation voltage of 200 kV. According to past literature, the tracks in c-Si were recrystallized with prolonged TEM observation [18]. Careful observations were performed to minimize the electron beam current and observation time.

3. Results

TEM images of c-Si irradiated with 9 MeV C_{60}^{2+} ions are exhibited in figure 2, where (a)–(c) and (d)(e) show irradiated pre-thinned and post-thinned samples, respectively. The observation angle of figure 2(a) was 0° from the surface normal but those of figures 2(b) and (c) were 30°. Figure 2(a) clearly exhibits many black dots, which are ascribed to the cross-sections of the tracks. The number density of the black dots was 4×10^{10} cm^{-2}, which is comparble to the ion fluence of 5×10^{10} cm^{-2}, confirming that the observed dots are ion tracks. The most of the tracks exhibit elliptical shapes, rather than true circles, with the major axes pointing the same direction. This could be due to the irradiation with an incident angle of 7° from the surface normal. With increasing the observation angle (i.e., tilting), the track images are divided into two parts; i.e. white circles and black rods, as

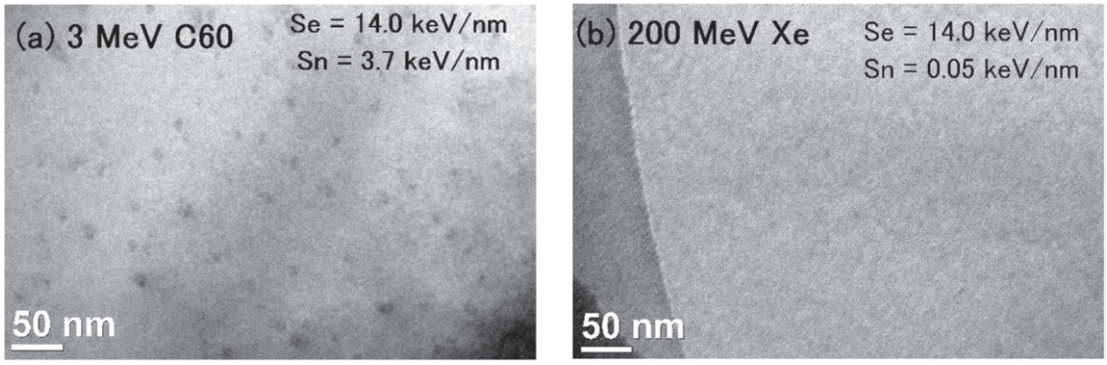

Figure 3. Bright field TEM images of pre-thinned c-Si samples irradiated with (a) 3 MeV C_{60}^{+} and (b) 200 MeV Xe^{14+} ions. (b) was reproduced with permission from [24] CC BY 4.0. The fluence was 5×10^{10} ions cm^{-2} for both the cases. Tracks are observed in (a) but not in (b). Both the irradiations have the same S_e, but different S_n.

shown in figures 2(b) and (c). They are observed as pairs in the most cases and are ascribed to the entrances and the main bodies of the tracks, respectively. Similar images were reported in YIG crystals irradiated with 40.2 MeV C_{60}^{3+} ions [27].

An interesting observation was that less modified region, i.e., a gap, existed between the white entrance and the black body. The same gaps were reported in YIG irradiated with 40.2 MeV C_{60}^{3+} ions [27], but not clear for c-Si irradiated with 30 MeV C_{60}^{2+} ions [18]. These gaps were observed in many tracks, and the mean width was roughly ~8 nm in the plane of the figure. Since the observation angle was 30°, the mean gap along the tracks was ~8 nm $\sin^{-1}(30°) = \sim 16$ nm. Figure 2(d) and (e) exhibit depth profiles of the tracks observed in the post-thinned samples. The gaps were not clearly observed in figure 2(d) and (e). This discrepancy has not been clarified yet. Possibly the gaps are due to the diffraction contrast, since the entrances and the bodies appear in white and black, respectively.

The mean track diameter under the 9 MeV irradiation was determined as 11.9 ± 1.7 nm, which is larger than that under 6 MeV irradiation. A decrease in the track radius with the ion energy, as expected in figure 1, was not observed.

4. Discussion

4.1. Involvement of S_n

Figure 3 compares TEM images of c-Si irradiated with (a) 3 MeV C_{60}^{+} ions and (b) 200 MeV Xe^{14+} ions. Both the ions have the same S_e of 14 keV nm^{-1} but much different S_n of 3.7 keV nm^{-1} and 0.05 keV nm^{-1} for 3 MeV C_{60} ion and 200 MeV Xe ion, respectively. The S_e of 14 keV nm^{-1} is much lower than the track formation threshold of ~30 keV nm^{-1} [16]. Even at the same value of S_e of 14 keVnm^{-1}, which is much lower than the threshold reported in past literature [16], the tracks were observed under 3 MeV C_{60} irradiation but not under 200 MeV Xe irradiation. This observation clearly indicates that there is another factor to control the formation of the ion tracks except S_e. Possible factors are the nuclear energy deposition S_n and the ion velocity. However, as shown in sub-section 4-3, the effect of the ion velocity is calculated by the i-TS model. It turns out that the difference in the ion velocity cannot explain the appearance/disappearance of the tracks.

Figure 4 shows S_e, S_n, and whether the tracks are formed or not, for six different ion species and energies at which the experiments were carried out. Track 'Yes' and 'No' in figure 4 denote the appearance and disappearance of the tracks, respectively. It is obvious from figure 4 that S_e is not a good indicator to decide whther the tracks are formed or not. While 3.6 GeV U ions have relatively high S_e, they do not form any tracks. Contrarty, 1 MeV C_{60} ions form ion tracks, although they have much lower S_e than 3.6 GeV U and even 200 MeV Xe ions. Rather S_n could be a better indicator: If we set a threshold value of S_n for track formation at, e.g., 0.5 keV nm^{-1}, all the experimental results in these six cases are explained without any exceptions. This fact may indicate that small but certain amount of S_n (>0.5 keV nm^{-1}) is a pre-requisite for the track formation in c-Si. Further discussion whether S_n is a better indicator or not is given in the next sub-section.

4.2. Closer involvement of S_e

As shown in figure 4, the S_n looks a good indicator whether the tracks are formed or not. However, the observed ion tracks (see figures 2(b)–(e)) show cylindrical shapes, not the nearly spherical shapes like collision cascades. This observation supports that the track formation is still governed by the S_e related processes. In fact, figure 5

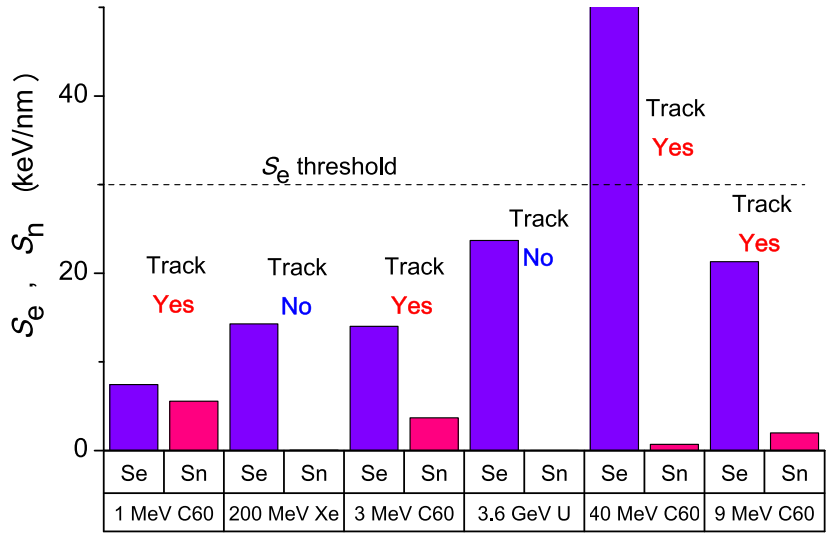

Figure 4. Values of S_e and S_n, and whether tracks are formed or not, are plotted for six different ion species and energies. The values of the monoatomic ions were calculated from SRIM 2013 [21] and those of the C_{60} ions were done from the equation (1) and SRIM 2013. Track 'Yes' and 'No' in the figure denote the appearance and the disappearance of the tracks, respectively.

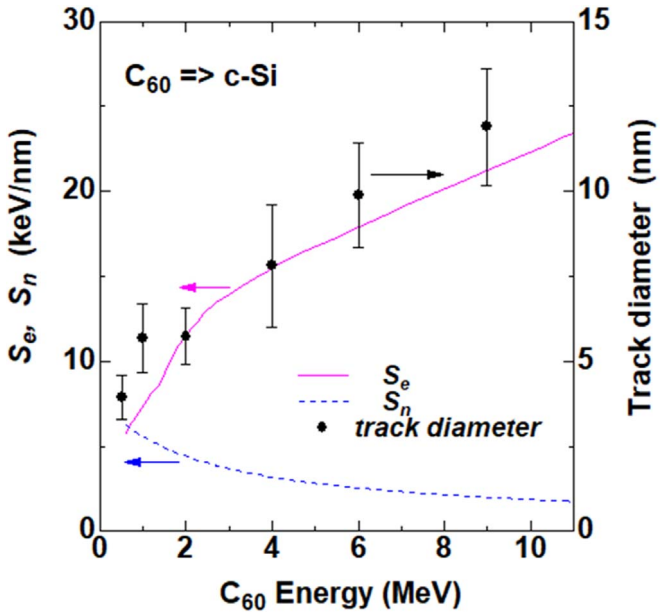

Figure 5. Ion energy dependences of electronic and nuclear energy deposition S_e and S_n in c-Si with C_{60} ions, which were calculated with equation (1) and SRIM 2013 [21]. The dependence of the track diameter is indicated by circles with error bars.

shows the energy dependences of S_e and S_n in c-Si irradiated with C_{60} ions, which were calculated by equation (1), in addition to the dependence of the mean track diameter. In the energy region between 1 and 10 MeV, where most of our experiments were conducted, S_n decrease but S_e increases with the ion energy. The mean track diameter also increases with the energy. As shown in figure 4, certain amounts of S_n is indispensable to the track formation. However, figure 5 shows that an increase of S_n (with decreasing E) results in the decrease of the track diameter. Rather the track diameter increases similarly with S_e.

We consider that the track formation itself is governed by the S_e-related processes as similar as the conventional SHI irradiations. However, a certain amounts of S_n is required to activate track formation processes or to protect tracks against the track-annihiration processes such as recrystallization.

4.3. Explanation from the Inelastic Thermal Spike Model

How does the i-TS model explain the quite high threshold (~30 keV nm^{-1}) of the track formation in c-Si ? Chettah *et al* calculated the radii of the molten tracks and of the vaporized tracks in c-Si induced by the i-TS

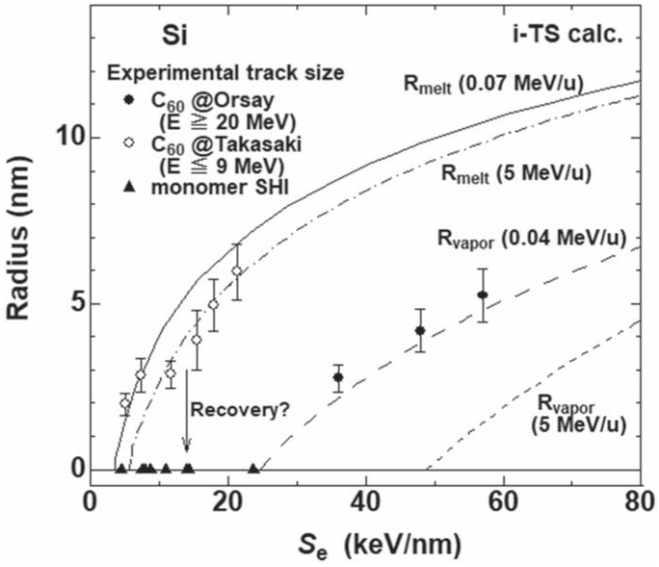

Figure 6. Electronic stopping power dependence of the radii of the melting regions and of the vaporized regions calculated by the inelastic thermal spike (i-TS) model [28]. The mean radii of the tracks formed in Orsay and those in this study are indicated by closed and open circles, respectively. Closed triangles indicate the results of monoatomic swift heavy ion (SHI) irradiations [13–15, 24] including 3.5 GeV Xe, 3.6 GeV U, and 200 MeV Xe ions, neither of which was successful in forming tracks.

effects for various S_e values [28], and compared them with those of the ion tracks observed under 20–40 MeV C_{60} irradiations. As shown in figure 6, the melting curves were plotted for two different velocities of 0.07 MeV/u and 5 MeV/u, and the vaporization curves for 0.04 MeV/u and 5 MeV/u. In these calculations, the velocity effect is taken into account. From the calculations, the threshold value for the melting transition was estimated to 3.5 keV nm^{-1} and 5.7 keV nm^{-1} for the velocities of 0.07 MeV/u and 5 MeV/u, respectively. Those of the vaporization transition was estimated to 25 keV nm^{-1} and 48 keV nm^{-1} for the velocities of 0.04 MeV/u and 5 MeV/u, respectively.

Most of the swift heavy monoatomic ion (SHMI) irradiations have carried out at the S_e values lower than 24 keV nm^{-1}, as indicated by closed triangles in figure 6. This is because S_e of ~24 keV nm^{-1} was attained under irradiation of GeV U ions which are the heaviest (quasi) stable ions. They are close to the Bragg maximum of S_e, i.e., the highest available S_e value in c-Si. Meanwhile, the experiments indicated that no ion tracks are formed in c-Si with any SHMI irradiations at S_e ~24 keV nm^{-1} or lower as indicated by the triangles in figure 6. However, the i-TS calculations indicate that the melting region is formed even at the S_e values higher than ~4 keV nm^{-1} for the veolocity of 0.07 MeV/u. This discrepancy between the experiments and the i-TS calculations can be solved if we assume the annihilation of the tracks. In fact, Chadderton proposed perfect expitaxial recrystallization of the molten tracks in c-Si [29], since efficient recrystallization was also observed in c-Si under low energy ion irradiation [29]. In this model, the molten tracks are formed in c-Si by SHMIs. After the formation of the molten regions by the SHMI irradiation, the molten regions recover by the perfect epitaxial recrystallization in c-Si. Therefore, when c-Si is irradiated with SHMIs, the molten regions are transiently formed but they are perfectly recrystallized with cooling. Ion tracks are no longer observed after then.

However, the ion track formation has been already reported in c-Si with C_{60} irradiations in Orsay [16, 18, 22]. In this case, high energies of 20, 30, and 40 MeV were applied. As indicated by closed circles in figure 6, the relationship between the track radius and S_e matched with the radii of the vaporized regions, rather than those of the molten regions. It indicates that the tracks observed in c-Si are formed via the vaporization, but not the melting. Even with the highly efficient recrystallization in c-Si, the perfect recovery of the vaporized regions are difficult. Consequently, the ion tracks were observed under high energy C_{60} irradiation performed at Orsay (20–40 MeV).

What happens under C_{60} irradiations in the energy regions between 1 and 9 MeV ? The data of the track radii versus S_e in the energy of 1–9 MeV are plotted by open circles in figure 6. Surprisingly these data points well fall on the curve of the radii of the molten regions. Therefore, the track formation under 1–9 MeV C_{60} irradiation can be ascribed to the molten transition in c-Si by the i-TS effects. Up to now, no data except ours fall on the radii of the molten regions because of the highly efficient recrystallization. We consider that the certain amount of S_n obstructs the efficient recrystallization in c-Si, while details have not been clarified. Using Rutherford backscattering spectrometry (RBS), Shen *et al* studied damage in c-Si irradiated with C_{60} ions of 100–530 keV, in which S_n of C_{60} ion reaches a maximum [30]. They observed that the damage was strongly enhanced by the

cluster effect: comparing with a carbon monomer ion of the same velocity (8.8 keV), C_{60} ion of 530 keV generated 7700 times more displacements and reduced the displacement energy [30], indicating the formation of the spikes. Such nuclear disorder could obstruct the recrystallization and enhace the survival ratio of the tracks in c-Si. According to our 9 MeV C_{60} irradiation to c-Si, the track areal density (4×10^{10} tracks cm^{-2}) was comparable to the ion fluence (5×10^{10} ions cm^{-2}) , indicating the track survival ratio of almost unity.

As mentined in sub-section 4-1, 200 MeV Xe irradiation does not form the tracks in c-Si but 3 MeV C_{60} irradiation does, while both the irradiations have the same S_e. The second governing factor could be S_n or the ion velocity. In fact, the velocity effect on the track sizes was calculated and shown in figure 6 for the melting transition at 5 MeV/u and 0.07 MeV. The difference between the curves at 5 MeV/u and 0.07 MeV/u is rather small and difficult to explain the apparence/disappearance of the tracks.

While the tracks are formed in both the energy regions of 1–9 MeV and 20–40 MeV, the properties of the tracks in the two regions can be different with each other. As mentioned with figure 1, the S_e dependence of the track radii formed in Orsay and that in Takasaki do not overlap with each other. This difference could be ascribed to the different properties of the track formation in 1–9 MeV and 20–40 MeV. Recently, Länger *et al* [31] reported negative evidence on the recrystallization of the tracks in c-Si under 1.14 GeV U ion irradiation. At the moment, we have no idea to merge it with our model.

4.4. Categorization of the synergy effects for track fromation

Following the discussion up to the previous sub-section, we have come to a conclusion that the track formation in c-Si under 1–9 MeV C_{60} ion irradiation requires both S_e and S_n for generating molten regions and reducing the recrstallization of the tracks, respectively. Therefore, the tracks in the present case are formed by a synergy effect between S_e and S_n. Up to now, various synergy effects between S_e and S_n have been reported [3, 10–12]: Here we discuss the syergy effect influencing the track formation only, with help of the i-TS theory. We don't discuss the recovery of point defects by S_e [10].

The i-TS model is described by coupled heat diffusion equations for the electronic and the atomic subsystems as shown in equations (3*a*) and (3*b*), where C_i, K_i, T_i , and A_i (i = e, a) denote the specific heat, thermal conductivity, temperature, and source term in the electronic (i = e) and atomic (i = a) subsystems, respectively. These two equations are bound by the electron-lattice coupling G. The point defect density plays an important role, which is assumed to mostly depend on S_n and the fluence Φ, as shown in equation (3*c*).

$$C_e(n_d)\frac{\partial T_e}{\partial t} = \nabla \cdot (K_e(n_d)\nabla T_e) - G(n_d)(T_e - T_a) + A_e(S_e) \tag{3a}$$

$$C_a(n_d)\frac{\partial T_a}{\partial t} = \nabla \cdot (K_a(n_d)\nabla T_a) + G(n_d)(T_e - T_a) + A_n(S_n) \tag{3b}$$

$$n_d = n_d(S_n,\ (S_e),\ \Phi) \tag{3c}$$

$$R_{tr} = R_{tr}(T_a(r),\ F_{recryst}(S_n,\ (S_e))) \tag{3d}$$

Since the point defect density n_d is reduced [10] or enhanced under high S_e, the density n_d also depends on S_e. However, this effect is not considered here. All the quantities C_i (n_d), K_i (n_d), (i = e, a) and G (n_d) are assumed to depend on n_d. While it is not described explicitly in literature, the mean track radius R_{tr} is a function of the spatial distribution of the atomic temperature T_a(r), as shown in equation (3*d*).

Because the mean track radius R_{tr} is reduced under efficient recrystallization, it is also the function of the recrystallization efficency $F_{recryst}$. Since the purpose of the equations is to show conceptial categorization of the different sources of the synergy effects, the mathematical completeness of these eqations is not discussed here.

Three types of the synergy effects are known as shown in table 1: the first type of the synergy effect is known as the pre-damage effect. It is known that previously introduced nuclear collisional damage enhances the i-TS effect, which results in formation of larger tracks than those without the pre-damage [11]. This effect is explained from equations (3*a*–3*d*), since K_e, K_a and G are the function of n_d. The increase in n_d turns to the decrease in the thermal conductivities K_a and probably K_e. Consequently the deposited energy from the ion is confined in smaller region, which results in higher maximum temperature than without the pre-damage. Also the increase in n_d turns to the increase in the coupling G, which results in more efficient energy transfer from the electronic to the atomic subsystem before the energy diffusion in the electronic subsystem. However, this type of the effects cannot explain the present phenomenon, since our target material Si was a single crystal before the C_{60} irradiation. Also the fluence was so low that overlaps of the tracks were negliglble. Therefore the 'pre-damage' does not exist in the present case. The 'pre-damage' mechanism is excluded. (However, if the i-TS heating by one ion is enhanced with the nuclear damage by the same ion, i.e., in situ-damage, the conclusion may change.)

The second type is the collateral heating of S_e and S_n, i.e., the unified thermal spike (u-TS) model: in the conventional i-TS model for SHIs, the energy from the ion was deposited to the electronic subsystem only, because the source term for the atomic subsystem, $A_n(S_n)$ in equation (3*b*), was excluded. The second synergy effect, i.e., the u-TS, is induced with the inclusion of the nuclear source term $A_n(S_n)$.

Table 1. Three mechanisms of the synergy effects between S_e and S_n for ion track formation.

Name of the synergy effect	Parameters playing roles	Mechanism	Inconsistency with the present phenomenon	References
Pre-damage effect	K_a, K_e and G	Damage introduced in the sample before the ion irradiation reduces the thermal conductivity K_a, which results in localization of heat near the track. Damage also enhances the electron-phonon coupling G. Both increase the lattice temperature of tracks compared with the non-damaged case.	Because of the low fluence, overlaps of tracks are negligible. Therefore, the pre-damage does not exist.	[11, 23]
Unified thermal spike (u-TS)	$A_n(S_n)$	In the i-TS model, only the electronic subsystem is heated by ions via $A_e(S_e)$. The atomic subsystem is indirectly heated via the coupling G. In the u-TS, the atomic subsystem is also directly heated via $A_n(S_n)$.	The nuclear heating effect A_n increases with S_n. As shown in figure 5, the track radii, however, increase with decreasing S_n. The observed energy dependence cannot be explained by the present effect.	[3]
Recrystalization of tracks	$F_{recryst}$	In Si, once-formed-tracks are easily annihilated by recrystalization. Because of high S_n, C_{60} ion irradiation introduces high concentration of defects, which obstruct the recrystallization. Therefore, certain portion of the tracks are survived and are observed.	No inconsistency.	This work

The nuclear heating effect A_n increases with S_n. However, the observed dependence on the track radii was opposed to the expectation. As shown in figure 5, S_n decreases with increasing the ion energy and the track radii increase with decreasing S_n. In fact, while we have carried out preliminary calculations with the unified thermal spike model [3], the energy dependence of the track radii as shown in figure 5 was not reproduced.

In the third type, the mean track radius is determined from not only the spatial profile of the atomic temperature but also the efficiency of the recrystallization $F_{recryst}$. The efficiency $F_{recryst}$ is a function of S_n and probably of S_e. While the details of this model have not been clarified yet, this model explains, at the moment, the present phenomenon better than others. While c-Si was believed as a radiation-hard material in the S_e regime with high S_e threshold, this study suggests that c-Si has a low S_e threshold but with efficient recrystallization.

5. Conclusions

It is known that no monoatomic SHIs can form ion tracks in c-Si. Exceptions were C_{60} cluster ion irradiation of 20–40 MeV, either of which provides much higher electronic energy deposition than any monoatomic SHIs. Since the mean track diameter decreased with decreasing the ion energy from 40 to 20 MeV, it was expected from an extrapolation that no tracks could been formed below the threshold of $S_{e,th} \sim 30$ keV nm^{-1} ($E_{th} \sim 17$ MeV). Nevertheless, we have observed that the tracks are formed under 1–9 MeV C_{60} ion irradiations, all of which are much lower than the extrapolated threshold of ~17 MeV. In this paper, some attempts were made to understand this phenomenon. Track formation was compared between irradiations of 200 MeV Xe ions and 3 MeV C_{60} irradiation, both of which have the same electronic stopping S_e of 14 keV nm^{-1} but much different nuclear stopping S_n of 0.05 keV nm^{-1} and 3.7 keV nm^{-1}, respectively. Tracks were only observed under 3 MeV C_{60} irradiation, which indicates the involvement of S_n for the track formation, i.e., the synergy effect. The results were compared with the i-TS calculations, which have clarified that the velocity effect does not play major roles. According to the i-TS calculations, the track formation under 20–40 MeV C_{60} irradiation is ascribed to the vaporization in c-Si, while the track formation via the melting transition, which is accessible by monoatomic SHI irradiation, has never been observed probably due to the quick recovery of the tracks by efficient recrystallization in c-Si. Collisional damage due to a certain amount of S_n under 1–9 MeV C_{60} irradiation disturbs the recrystallization of c-Si, which results in the survival of the tracks formed by the melting transitions. Since this mechanism is different from the known synergy effects of the pre-damage effect and the u-TS, this can be a new type of the synergy effect between S_e and S_n for track formation. While c-Si was believed as a radiation-hard material in the S_e regime with high S_e threshold, this study suggests that c-Si has a low S_e threshold but with efficient recrystallization.

Acknowledgments

A part of the study was supported by the Inter-organizational Atomic Energy Research Program through an academic collaborative agreement among JAEA, QST, and Univ. of Tokyo. The authors are grateful to the crew of the accelerator facilities at QST-Takasaki and at JAEA-Tokai for their help. HA was supported by JSPS-KAKENHI Grant number 22K04990. TEM observation was performed using the facility of the NIMS TEM station.

Data availability statement

The data that support the findings of this study are available upon reasonable request from the authors.

Authors contributions

A C, Y H, K Y, K N, and Y S have developed the MeV high-flux C_{60} ion beam. H A prepared samples. Y S, A C, Y H, S Y and K N conducted C_{60} ion irradiation. N I and N O conducted 200 MeV Xe irradiation. H A conducted TEM observation. M T supplied information on the past literature and valuable suggestions. All the authors joined in discussion of the results and contributed to manuscript preparation.

Additional information

No supplementary information is attached.

Competing interests

The authors declare no competing interests.

ORCID iDs

H Amekura https://orcid.org/0000-0003-2148-8431
S Yamamoto https://orcid.org/0000-0003-0407-0033
N Ishikawa https://orcid.org/0000-0002-2217-3645

References

[1] Avasthi D K and Mehta G K 2011 *Swift Heavy Ions for Materials Engineering and Nanostructuring* (Berlin, Heidelberg, New York: Springer)
[2] Amekura H, Chen F and Jia Y 2020 *Ion Irradiation of Dielectrics for Photonic Applications* (Singapore: Springer Nature) Chap. 5
[3] Toulemonde M, Weber W J, Li G, Shutthanandan V, Kluth P, Yang T, Wang Y and Zhang Y 2011 Synergy of nuclear and electronic energy losses in ion-irradiation processes: the case of vitreous silicon dioxide *Phys. Rev. B* **83** 054106
[4] Young D A 1958 Etching of radiation damage in lithium fluoride *Nature* **182** 375
[5] Silk E C H and Barnes R S 1959 Examination of fission fragment tracks with an electron microscope *Philos. Mag.* **4** 970
[6] Itoh N, Duffy D M, Khakshouri S and Stoneham A M 2009 Making tracks: electronic excitation roles in forming swift heavy ion tracks *J. Phys. Condens. Matter* **21** 474205
[7] Wesch W and Wendler E (ed) 2016 *Ion Beam Modification of Solids - Ion-Solid Interaction and Radiation Damage* (Basel, Switzerland: Springer International Publishing) 61
[8] Dufour C and Toulemonde M 2016 *Ion Beam Modification of Solids* ed W Wesch and E Wendler (Basel, Switzerland: Springer International Publishing) 63
[9] Rymzhanov R A, Medvedev N, O'Connell J H, Janse van Vuuren A, Skuratov V A and Volkov A E 2019 Recrystallization as the governing mechanism of ion track formation *Sci. Rep.* **9** 3837
[10] Zinkle S J, Skuratov V A and Hoelzer D T 2002 On the conflicting roles of ionizing radiation in ceramics *Nucl. Instrum. Methods Phys. Res., Sect. B* **191** 758
[11] Weber W J, Zarkadoula E, Pakarinen O H, Sachan R, Chisholm M F, Liu P, Xue H, Jin K and Zhang Y 2015 Synergy of elastic and inelastic energy loss on ion track formation in $SrTiO_3$ *Sci. Rep.* **5** 7726
[12] Thomé L, Debelle A, Garrido F, Trocellier P, Serruys Y, Velisa G and Miro S 2013 Combined effects of nuclear and electronic energy losses in solids irradiated with a dual-ion beam *Appl. Phys. Lett.* **102** 141906
[13] Toulemonde M, Dural J, Nouet G, Mary P, Hamet J F, Beaufort M F, Desoyer J C, Blanchard C and Auleytner J 1989 High energy heavy ion irradiation of silicon *Physica Status Solidi (a)* **114** 467
[14] Mary P, Bogdanski P, Nouet G and Toulemonde M 1989 Defects created by 3.5 GeV xenon ions in silicon *Appl. Surf. Sci.* **43** 102
[15] Mary P, Bogdanski P, Toulemonde M, Spohr R and Vetter J 1992 Deep-level transient spectroscopy studies of U-irradiated silicon *Nucl. Instrum. Methods Phys. Res., Sect. B* **62** 391
[16] Colder A, Canut B, Levalois M, Marie P, Portier X and Ramos S M M 2002 Latent track formation in GaAs irradiated with 20, 30, and 40 MeV fullerenes *J. Appl. Phys.* **91** 5853
[17] Furuno S, Otsu H, Hojou K and Izui K 1996 Tracks of high energy heavy ions in solids *Nucl. Instrum. Methods Phys. Res., Sect. B* **107** 223
[18] Dunlop A, Jaskierowicz G and Della-Negra S 1998 Latent track formation in silicon irradiated by 30 MeV fullerenes *Nucl. Instrum. Methods Phys. Res., Sect. B* **146** 302
[19] Srivastava P C, Ganesan V and Sinha O P 2002 AFM study of swift gold ion irradiated silicon *Nucl. Instrum. Methods Phys. Res., Sect. B* **187** 220
[20] Bouneau S, Brunelle A, Della-Negra S, Depauw J, Jacquet D, Le Beyec Y, Pautrat M, Fallavier M, Poizat J C and Andersen H H 2002 Very large gold and silver sputtering yields induced by keV to MeV energy Au_n clusters ($n = 1$–13) *Phys. Rev. B* **65** 144106
[21] Ziegler J F, Biersack J P and Ziegler M D 2008 *SRIM - The Stopping and Range of Ions in Matter* (Chester, MD, USA: SRIM Co.)
[22] Canut B, Bonardi N, Ramos S M M and Della-Negra S 1998 Latent tracks formation in silicon single crystals irradiated with fullerenes in the electronic regime *Nucl. Instrum. Methods Phys. Res., Sect. B* **146** 296
[23] Kamarou A, Wesch W, Wendler E, Undisz A and Rettenmayr M 2008 Radiation damage formation in InP, InSb, GaAs, GaP, Ge, and Si due to fast ions *Phys. Rev. B* **78** 054111
[24] Amekura H *et al* 2021 Ion tracks in silicon formed by much lower energy deposition than the track formation threshold *Sci. Rep.* **11** 185
[25] Chiba A, Usui A, Hirano Y, Yamada K, Narumi K and Saitoh Y 2020 Novel approaches for intensifying negative C_{60} ion beams using conventional ion sources installed on a tandem accelerator *Quantum Beam Science* **4** 13
[26] Amekura H, Narumi K, Chiba A, Hirano Y, Yamada K, Yamamoto S and Saitoh Y 2022 Incident angle dependent formation of ion tracks in quartz crystal with C_{60}^{+} ions: big ions in small channels *Quantum Beam Science* **6** 4
[27] Dunlop A, Jaskierowicz G, Jensen J and Della-Negra S 1997 Track separation due to dissociation of MeV C_{60} inside a solid *Nucl. Instrum. Methods Phys. Res., Sect. B* **132** 93
[28] Chettah A, Kucal H, Wang Z G, Kac M, Meftah A and Toulemonde M 2009 Behavior of crystalline silicon under huge electronic excitations: a transient thermal spike description *Nucl. Instrum. Methods Phys. Res., Sect. B* **267** 2719
[29] Chadderton L T 2003 Nuclear tracks in solids: registration physics and the compound spike *Radiat. Meas.* **36** 13
[30] Shen H, Brink C, Hvelplund P, Shiryaev S, Shi P and Davies J A 1997 Fullerene ion (C_{60}^{+}) damage in Si at 25 °C *Nucl. Instrum. Methods Phys. Res., Sect. B* **129** 203
[31] Länger C, Ernst P, Bender M, Severin D, Trautmann C, Schleberger M and Dürr M 2021 Single-ion induced surface modifications on hydrogen-covered Si(001) surfaces—significant difference between slow highly charged and swift heavy ions *New J. Phys.* **23** 093037